# A method for generalized sampling and reconstruction of finite-rate-of-innovation signals

Chandra Sekhar Seelamantula and Michael Unser
Biomedical Imaging Group
Ecole polytechnique fédérale de Lausanne
Switzerland
{chandrasekhar.seelamantula, michael.unser}@epfl.ch

**Abstract:**

We address the problem of generalized sampling and reconstruction of finite-rate-of-innovation signals. Specifically, we consider the problem of sampling streams of Dirac impulses and propose a two-channel method that enables fast, local reconstruction under some suitable conditions. We also specify some acquisition kernels and give the associated reconstruction formulas. It turns out that these kernels can also be combined into one kernel, which can be employed in the single-channel sampling scenario. The single-kernel approach carries over all the advantages of the two-channel counterpart. Simulation results are presented to validate the theoretical calculations.

## 1. Introduction and prior art

Sampling theory is the foundation on which digital signal processing has been built. The popular flavor of the sampling theory is due to Shannon [1] and deals exclusively with bandlimited signals. Shannon's theory was generalized in several ways, the most prominent one being the theory of multichannel sampling developed by Papoulis [3]—his theory is known as the Generalized Sampling Theory. Papoulis' formalism, however, deals only with bandlimited signals. To accommodate the more general class of finite-energy signals, Unser and Zerubia [4] developed a theory, which does not rely on the bandlimiting constraint. Another important extension is the sampling and reconstruction of signals that lie in some shift-invariant subspace spanned by the integer-shifted versions of a generator kernel (see [2] and the references therein). The specific case of bandlimited sampling corresponds to a sinc kernel and is subsumed by this formalism.

Recently, Vetterli *et al.* [5] extended sampling theory in a new direction to answer a question that has not been addressed before—that of sampling and reconstructing streams of Dirac impulses and signals derived therefrom. These signals are not constrained to lie in the space of finite-energy functions nor in the space of bandlimited functions. They may also not lie in some shift-invariant subspace generated by a kernel. Typically, such signals are specified by a set of discrete parameters per time unit, also known as their rate of innovation. We are interested in signals that have a finite rate of innovation (FRI). Specifically, consider the stream of time-ordered Dirac impulses:

$$x(t) = \sum_{\ell=1}^{L} a_\ell \delta_D(t - t_\ell), \tag{1}$$

where $\delta_D(\cdot)$ denotes the Dirac impulse. The problem is to compute the parameters $\{a_\ell, t_\ell; 1 \leq \ell \leq L\}$ based on some measurements on $x(t)$. The parametric nature of the problem has resulted in the development of techniques that are quite different from those that sampling theorists have been familiar with. Typically, the reconstruction techniques developed by Vetterli *et al.* [5] and Dragotti *et al.* [6] have a flavor of parametric spectral estimation [7]. They also employ in a novel fashion spline kernels [8, 9] that reproduce polynomials or exponentials. It is remarkable that these kernels, which play a vital role in wavelet theory, are also quite useful for sampling FRI signals.

In the techniques mentioned above, the focus is exclusively on the single-channel case. Recently, some new multichannel approaches have also been developed. Kusuma and Goyal proposed a new technique for reconstructing an unknown number of impulses over a finite interval of time by using a successive approximation criterion [10]. Their technique can be implemented using a bank of integrators and B-splines. Baboulaz and Dragotti proposed a distributed acquisition scheme for FRI signals and demonstrated applications to image registration and super-resolution image restoration [11]. In [12], we have proposed a two-channel sampling method for the FRI problem (cf. Fig. 1). We have employed first-order resistor-capacitor networks to sample streams of Dirac impulses and piecewise-constant functions. The reconstruction technique boils down to solving a system of two equations containing the unknown parameters in decoupled form. The key result in [12] is given below:

**Proposition 1** *The stream of Dirac impulses in* (1) *is uniquely specified by the samples* $y_\alpha(nT) = (x * h_\alpha)(nT)$ *and* $y_\gamma(nT) = (x * h_\gamma)(nT)$, $n \in \mathbb{Z}$, *where* $h_\alpha(t) = \alpha\, e^{-\alpha t} u(t)$, $h_\gamma(t) = \gamma\, e^{-\gamma t} u(t)$, *and* $\alpha \neq \gamma$, *provided that* $\min_{2 \leq \ell \leq L} \{t_\ell - t_{\ell-1}\} \geq T$.

### 1.1 Motivation for the present work

The above proposition relies on causal exponential functions for sampling. Working with exponentials has the practical advantage that they can be easily generated by employing first-order resistor-capacitor circuits. From a mathematical viewpoint, however, exponentials are probably not the only class of functions that enable accurate reconstruction. The main motivation behind the present paper is the quest for alternative kernels $h_\alpha(t)$ and $h_\gamma(t)$ that would fit into the framework of the above proposition (also cf. Fig. 1). To that end, we first reformulate the method proposed in [12] in a more general framework and specify some kernels that enable exact reconstruction.

## 2. Generalized sampling formulation

Consider the two-channel sampling scenario shown in Fig. 1. Let $h_\alpha(t)$ and $h_\gamma(t)$, $\alpha, \gamma \in \mathbb{C}$, denote the impulse responses of two causal linear shift-invariant systems, compactly supported on $[0, T]$ and nonzero over that interval. Consider the stream of Dirac impulses in (1), where the impulses are separated by at least $T$; i.e.,

$$\min_{2\leq \ell \leq L} \{t_\ell - t_{\ell-1}\} \geq T. \tag{2}$$

Deviations from this condition shall be addressed later. The output of the system to the input $x(t)$ is given by

$$y_\alpha(t) \triangleq (x * h_\alpha)(t) = \sum_{\ell=1}^{L} a_\ell h_\alpha(t - t_\ell).$$

Let us next consider the samples of $y_\alpha(t)$ taken on a uniform grid with a sampling step $T$. Note that we have chosen the sampling period to be equal to the support of $h_\alpha(t)$; otherwise, we are likely to miss some closely-spaced impulses as the following analysis shows. The samples of $y_\alpha(t)$ are given by

$$y_\alpha(nT) = \sum_{\ell=1}^{L} a_\ell \, h_\alpha \left(nT - t_\ell\right) \delta_K \left[nT - r(t_\ell)\right],$$

where $r(t_\ell) = \left\lceil \frac{t_\ell}{T} \right\rceil T$ is the operator that performs the ceiling of $t_\ell$ with respect to the sampling grid and $\delta_K$ denotes the Kronecker impulse. The sequence $y_\alpha(nT)$ comprises Kronecker impulses, each corresponding to a Dirac impulse in $x(t)$ under the condition (2). Note that the sampling period $T$ equals the support of the kernel. Similarly, corresponding to a system with impulse response $h_\gamma(t)$, $\gamma \neq \alpha$, we have

$$y_\gamma(nT) = \sum_{\ell=1}^{L} a_\ell \, h_\gamma \left(nT - t_\ell\right) \delta_K \left[nT - r(t_\ell)\right].$$

Note that these sampling instants correspond to the nonzero values in the sequences $y_\alpha(nT)$ and $y_\gamma(nT)$ and are therefore known. Consider the $\ell^{th}$ nonzero samples in the sequences $y_\alpha(nT)$ and $y_\gamma(nT)$:

$$y_\alpha(r(t_\ell)) = a_\ell \, h_\alpha[r(t_\ell) - t_\ell] \text{ and} \tag{3}$$
$$y_\gamma(r(t_\ell)) = a_\ell \, h_\gamma[r(t_\ell) - t_\ell]. \tag{4}$$

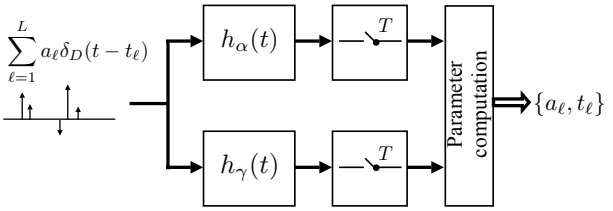


Figure 1: Two-channel sampling of a stream of dirac impulses.

In (3) and (4), the indices $r(t_\ell)$ and the values on the left hand side are known. The impulse responses $h_\alpha$ and $h_\gamma$ are also known; their design shall be explained below. The amplitude and position parameters $\{t_\ell, a_\ell\}$ are unknown and have to be determined. The amplitude of the $\ell^{th}$ Dirac impulse appears as a multiplicative factor. The position of the Dirac impulse is encoded in the amplitude of the Kronecker impulse. Dividing (3) by (4) eliminates $a_\ell$ and gives rise to an equation in the unknown $t_\ell$, which can be computed if and only if $(h_\alpha / h_\gamma)(t)$ is invertible on its range. The value of $t_\ell$ thus obtained can then be substituted in (3) or (4) to obtain the value of $a_\ell$. Some specific functions that fit into the above reconstruction paradigm are presented next.

## 3. Kernels for two-channel sampling

We specify only the kernel $h_\alpha(t)$; unless otherwise mentioned, $h_\gamma(t)$ is obtained by replacing $\alpha$ with $\gamma$; i.e., both kernels have the same functional form. The kernels involve gating by the B-spline of order zero, at scale $T$: $\beta(t) = u(t) - u(t - T)$, where $u(t)$ is the unit step function. We specify the kernel definitions and give the expressions for $\{t_\ell, a_\ell\}$ directly. The intermediate calculations are omitted but it is straightforward to supply them starting from the definition of the kernel.

1. Exponential spline (E-spline) kernels [9]: $h_\alpha(t) = e^{-\alpha t}\beta(t), \alpha \in \mathbb{R}$, where $u(t)$ is the unit-step function. The parameters of $\ell^{th}$ impulse are given by

$$t_\ell = r(t_\ell) + \frac{1}{\alpha - \gamma} \log\left(\frac{y_\alpha(r(t_\ell))}{y_\gamma(r(t_\ell))}\right) \text{ and}$$
$$a_\ell = y_\alpha(r(t_\ell)) \exp\left(-\frac{\alpha}{\alpha - \gamma} \log\left(\frac{y_\alpha(r(t_\ell))}{y_\gamma(r(t_\ell))}\right)\right).$$

   This kernel choice has been analyzed in sufficient detail in [12]. The specific kernel given above is a first-order E-spline kernel. One could, in principle, also employ higher-order kernels. The advantage of first-order E-spline kernels over the higher-order ones, however, is that they always give rise to closed-form solutions. The higher-order kernels exhibit this property only for certain values of the spline parameters. For further discussion on this issue, we refer the reader to [12].

2. Power functions: $h_\alpha(t) = t^\alpha \beta(t)$, $\alpha \in \mathbb{R}$. Corre-

spondingly, the parameters of $x(t)$ are given by

$$t_\ell = r(t_\ell) - \left(\frac{y_\alpha(r(t_\ell))}{y_\gamma(r(t_\ell))}\right)^{\frac{1}{\alpha-\gamma}} \text{ and}$$
$$a_\ell = y_\alpha(r(t_\ell)) \left(\frac{y_\alpha(r(t_\ell))}{y_\gamma(r(t_\ell))}\right)^{\frac{-\alpha}{\alpha-\gamma}}.$$

For $\alpha \in \mathbb{Z}^+$, the power function becomes a monomial of degree $\alpha$. Since B-splines of order $\alpha$ can reproduce polynomials (and naturally, monomials too) up to degree $\alpha$, they are included as special elements of this class. Therefore, power functions, which play a vital role in moment-based sampling approaches [6, 11] for the FRI problem, are also useful in the generalized sampling approach. Also, note that fractional powers are admissible in the kernel definition.

3. Gaussian functions: $h_\alpha(t) = e^{-\alpha t^2}\beta(t)$, where $\alpha \in \mathbb{R}$. Correspondingly, we have that

$$t_\ell = r(t_\ell) - \sqrt{\frac{1}{\alpha-\gamma}\log\left(\frac{y_\gamma(r(t_\ell))}{y_\alpha(r(t_\ell))}\right)}, \text{and}$$
$$a_\ell = \exp\left(\frac{\alpha}{\alpha-\gamma}\log\left(\frac{y_\gamma(r(t_\ell))}{y_\alpha(r(t_\ell))}\right)\right).$$

4. Complex E-splines: $h_\alpha(t) = e^{-\mathrm{j}\alpha t}\beta(t)$, $\alpha \in \mathbb{R}$. This kernel cannot be treated as a special case of the E-spline kernels with an imaginary parameter. The reason is that there is an issue related to *parameter identifiability* that deserves special attention. The potential problem is that this kernel may give rise to more than one solution for $t_\ell$; there is, however, no ambiguity in the solution for $a_\ell$. We further explain this issue and also state a condition that helps overcome the non-uniqueness hurdle.
The cause of ambiguity is essentially the quasi-periodicity of the complex exponential over the support $[0, T]$:

$$e^{-\mathrm{j}\alpha\,(r(t_\ell)-t_\ell)} = e^{-\mathrm{j}\alpha\left(r(t_\ell)-t_\ell+\frac{2m\pi}{\alpha}\right)},$$

for $m \in \mathbb{Z}$ such that $0 \leq (r(t_\ell)-t_\ell+\frac{2m\pi}{\alpha}) \leq T$. The restriction on $m$ is due to the fact that we are considering a truncated complex exponential. The inequality gives rise to multiple solutions for $t_\ell$. The solution to this problem lies in tying up the choices of the values of $\alpha$ and $T$ such that $m = 0$ is the only possibility in the above inequality. This amounts to requiring that the complex exponential have at maximum one period within a sampling interval; i.e., $\frac{2\pi}{\alpha} > T$. Under this condition, we have the reconstruction formulae:

$$t_\ell = -\mathrm{j}\,\log\left(\frac{y_\alpha(r(t_\ell))e^{\mathrm{j}\alpha\, r(t_\ell)}}{y_\gamma(r(t_\ell))e^{\mathrm{j}\gamma\, r(t_\ell)}}\right), \text{and}$$
$$a_\ell = y_\alpha(r(t_\ell))\exp\left(\mathrm{j}\alpha(r(t_\ell)-t_\ell)\right).$$

Similarly, a truncated Fresnel kernel can be employed by considering purely imaginary parameters in the definition of the Gaussian above. For complex parameters, the E-spline and Fresnel kernels have an exponential and Gaussian decay, respectively.

5. Hybrid sampling kernels: In the kernels considered above, we have enforced the same functional form for both $h_\alpha(t)$ and $h_\gamma(t)$. By relaxing this property, we can make the reconstruction technique more efficient. For example, if we set one of the parameters (but not both), say $\alpha$ to zero, the kernel reduces to a causal B-spline of order 0: $h_\alpha(t) = \beta(t)$. The second kernel can be taken from any of the choices listed above. The samples from the zeroth-order B-spline channel then directly yield $a_\ell = y_\alpha(r(t_\ell))$. Using the samples from the second channel, we can compute the positions of the Dirac impulses. For example, if we employ the truncated power function in the second channel, we have that $t_\ell = r(t_\ell) - \left(\frac{y_\gamma(r(t_\ell))}{a_\ell}\right)^{\frac{1}{\gamma}}$. Note that $r(t_\ell)$ and $y_\gamma(r(t_\ell))$ are known.

Having listed a few kernel choices, we reiterate that, in the present formalism, the condition stated in (2) is crucial for the super-resolution localization of impulses. If two successive Dirac impulses are spaced closer apart than the sampling period, then they give rise to overlapping Kronecker impulses and resolving them is not possible within the proposed formulation. The existing approaches [5, 6, 10, 11] do not suffer from this limitation.

## 4. Kernels for single-channel sampling

The principal advantage offered by the two-channel method equipped with the choice of a proper kernel is the decoupling between the amplitudes and positions of the impulses. As shown next, this advantage can be carried over to the single-channel case by suitably integrating the previously listed kernels into a single function. For example, consider the kernel: $h_{\alpha,\gamma}(t) = e^{-\alpha t}\beta(t) + e^{-\gamma\,(t-T)}\beta(t-T)$, which has the same properties as the hybrid kernel in the two-channel case (kernel (1) in Section 3.). This choice would give rise to two nonzero samples per Dirac impulse, which can be used to solve for $a_\ell$ and $t_\ell$. Again, if $\alpha = 0$, the first sample would straightaway give the amplitude, which can then be used together with the second sample to compute the position. Thus, we have a similar algorithm as in the two-channel case, the only difference being that, in the two-channel case, these samples are acquired one per channel whereas in the one-channel case, they are acquired in the same channel—the overall sampling rate, however, is the same in both the cases. In general, the kernels for the single-channel case can be defined as: $h_{\alpha,\gamma}(t) = h_\alpha(t) + h_\gamma(t-T)$. Since the support of the kernel $h_{\alpha,\gamma}(t)$ is double that of $h_\alpha(t)$ or $h_\gamma(t)$, impulses that are farther apart by at least $2T$ $\Big($i.e., $\min\limits_{2\leq\ell\leq L}\{t_\ell - t_{\ell-1}\} \geq 2T\Big)$ only can be resolved. The kernels defined in this paper are shown in Fig. 2.

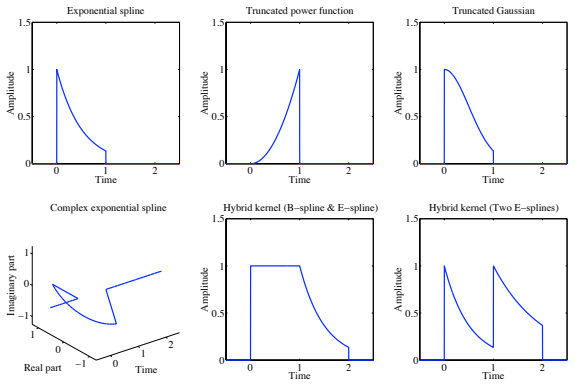


Figure 2: Sampling kernels. The parameters $\alpha = 2, \gamma = 1$, and $T = 1$, are chosen for the sake of illustration.

## 5. Simulations

We next validate the theoretical findings by numerical experiments. We simulate the two-channel sampling of nine Dirac impulses shown in Fig. 3(a); the amplitudes and positions are chosen for the purpose of illustration. The minimum spacing between two impulses is 0.0076 seconds. The sampling period $T$ is chosen to be $0.0038$ seconds to ensure that (2) is satisfied. The impulses are sampled using the power function kernels with parameters $\alpha = 3, \gamma = 2$, and $T = 0.0038$ seconds. These values are chosen for the purpose of illustration. The reconstructed stream of Dirac impulses is shown in Fig. 3(b). The reconstruction is accurate to numerical precision. Identical results were obtained with the other kernel choices.

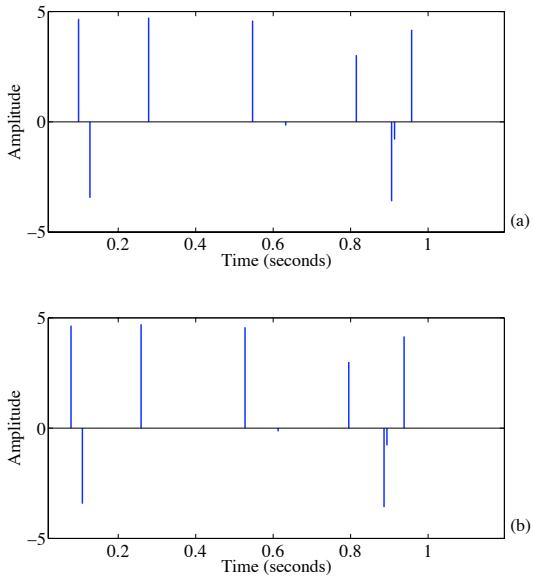


Figure 3: (a) Ground truth, (b) Reconstructed signal.

## 6. Conclusions

We have extended the results developed in [12] and proposed new kernels for both single-channel and two-channel sampling scenarios. The kernels are built using functions known in system theory such as the exponential, power function, Gaussian, etc. The main advantage of the proposed formulation is that, under the condition of minimum separation between consecutive impulses, a fast local reconstruction algorithm can be developed. This advantage, however, comes with the shortcoming that impulses spaced farther apart than the sampling period only can be resolved. It would be a challenging task to develop local reconstruction algorithms without imposing constraints on the minimum/average separation between impulses or groups thereof.

## Acknowledgments

This work was supported by the Swiss National Science Foundation (SNSF) Grant 200020-101821.

## References:

[1] C. E. Shannon, "Communication in the presence of noise," *Proc. IRE*, vol. 37, no. 1, pp. 10-21, Jan. 1949.

[2] M. Unser, "Sampling—50 years after Shannon," *Proc. IEEE*, vol. 88, no. 4, pp. 569-587, Apr. 2000.

[3] A. Papoulis, "Generalized sampling expansion," *IEEE Trans. Circuits Syst.*, vol. 24, no. 11, pp. 652–654, 1977.

[4] M. Unser and J. Zerubia, "A generalized sampling theory without band-limiting constraints," *IEEE Trans. Circuits Syst. II, Analog and Digit. Signal Process.*, vol. 45, no. 8, pp. 959–969, Aug. 1998.

[5] M. Vetterli, P. Marziliano, and T. Blu, "Sampling signals with finite rate of innovation," *IEEE Trans. Signal Process.*, vol. 50, no. 6, pp. 1417–1428, Jun. 2002.

[6] P.L. Dragotti, M. Vetterli, and T. Blu, "Sampling moments and reconstructing signals of finite rate of innovation: Shannon meets Strang-Fix," *IEEE Trans. Signal Process.*, vol. 55, no. 5, pp. 1741–1757, May 2007, Part 1.

[7] P. Stoica and R. Moses, *Introduction to Spectral Analysis*, Englewood Cliffs, NJ: Prentice-Hall, 2000.

[8] M. Unser, "Splines: A perfect fit for signal and image processing," *IEEE Signal Process. Mag.*, vol. 16, no. 6, pp. 22–38, Nov. 1999.

[9] M. Unser and T. Blu, "Cardinal exponential splines: Part I—Theory and filtering algorithms," *IEEE Trans. Signal Process.*, vol. 53, no. 4, pp. 1425–1438, Apr. 2005.

[10] J. Kusuma and V. K. Goyal, "Multichannel sampling of parametric signals with a successive approximation property," in *Proc. IEEE Intl. Conf. on Imag. Proc.*, 2006, pp. 1265–1268.

[11] L. Baboulaz and P. L. Dragotti, "Distributed acquisition and image super-resolution based on continuous moments from samples," in *Proc. IEEE Intl. Conf. on Imag. Proc.*, 2006, pp. 3309–3312.

[12] C. S. Seelamantula and M. Unser, "A generalized sampling method for finite-rate-of-innovation-signal reconstruction," *IEEE Signal Process. Lett.*, vol. 15, pp. 813-816, 2008.